Exploitation of the coffee-ring effect to realize mechanically enhanced inkjet-printed microelectromechanical relays with U-bar-shaped cantilevers

Seungjun Chung' , Muhammed Ahosan Ul Karim, Matthew Spencer, Hyuk-Jun Kwon, Costas P. Grigoropoulos, Elad Alon, and Vivek Subramanian

Citation: Appl. Phys. Lett. **105**, 261901 (2014); doi: 10.1063/1.4904953
View online: http://dx.doi.org/10.1063/1.4904953
View Table of Contents: http://aip.scitation.org/toc/apl/105/26
Published by the American Institute of Physics

APPLIED PHYSICS LETTERS **105**, 261901 (2014)

Exploitation of the coffee-ring effect to realize mechanically enhanced inkjet-printed microelectromechanical relays with U-bar-shaped cantilevers

Seungjun Chung,[1,a)] Muhammed Ahosan Ul Karim,[1] Matthew Spencer,[1] Hyuk-Jun Kwon,[2] Costas P. Grigoropoulos,[2] Elad Alon,[1] and Vivek Subramanian[1]
[1]*Department of Electrical Engineering and Computer Science, University of California, Berkeley, California 94720, USA*
[2]*Department of Mechanical Engineering, University of California, Berkeley, California 94720, USA*

(Received 15 October 2014; accepted 8 December 2014; published online 29 December 2014)

We report a mechanically enhanced inkjet-printed microelectromechanical (MEM) relay with a U-bar-shaped cantilever by exploiting the coffee-ring effect. The printed cantilever shape, especially the effective thickness caused by the elevated walls, can be controlled during the drying process by outward convective flow of silver nanoparticles. This enhances mechanical stiffness to efficiently produce a strongly suspended cantilever that is immune to collapse- and curling-related failures. This approach to enhancing cantilever stiffness is unique to printing-based processes using metal-nanoparticle inks and is not feasible for conventional photolithography processes. The resulting printed MEM relays show a pull-in voltage of only 6.6 V and an on/off ratio of 10^8 with extremely low on-state resistance ($\sim$14.3 Ω) and off-state leakage that is comparable to those of conventional silicon-based MEM relays. © *2014 AIP Publishing LLC*. [http://dx.doi.org/10.1063/1.4904953]

Printed electronics technology has attracted considerable interest for realizing low-cost, low-temperature, flexible, and large-area electronic systems such as thin-film transistors (TFTs) with uses in applications such as displays[1,2] and radio-frequency identification tags.[3,4] Although printed TFTs have shown drastically improved electrical characteristics in recent years,[5–7] further improvements are still needed with respect to their power-consumption, environmental stability, subthreshold swing, and on/off ratio. An alternative approach that is particularly attractive for applications requiring ultra-low device leakage is the use of printed microelectromechanical (MEM) relay with movable cantilevers operated by electrostatic actuation.[8,9] A semiconductor layer is not required in mechanical switching devices; therefore, extremely low on-state resistances and off-state leakage currents are normally observed. These devices also offer excellent stability since they are not significantly affected by environmental conditions. To realize high-performance printed MEM relays, strongly suspended cantilevers must be used as channels between the source and drain electrodes to prevent stiction and collapse during operation and sacrificial layer removal.[10,11] In addition, the cantilever beam should be controllable to have a suitable stiffness because an excessively stiff cantilever beam requires a high pull-in voltage (V_{PI}). Thus, many research groups have attempted to optimize the process conditions for realizing suspended cantilevers. For example, in conventional lithographically processed MEM relays, the geometric shape of the cantilever has been adjusted to tune effective stiffness[12,13] However, merely optimizing the thickness and length of printed cantilevers is insufficient to achieve viable devices due to the limitations of printable materials and printing resolution.[14] For example, it is very hard to obtain a printed electrode that is more than 10 μm thick because of ink-spreading and poor sintering of thick nanoparticle-based films.[15] Therefore, new approaches must be developed to enhance the mechanical stiffness of printed cantilever beams for use in high-performance and stable inkjet-printed MEM relays.

In this study, using an approach that uniquely exploits the physics of inkjet printing, a simple and efficient method exploiting the coffee-ring effect was developed to control the stiffness of printed cantilever beams. Many studies have been reported to reduce or eliminate the coffee-ring effect to obtain smooth and uniform surfaces.[16–18] In this work, we instead specifically exploit the coffee ring effect to form a stiff U-bar shaped beam. This phenomenon increases the effective height of the U-shaped beam to control the moment of inertia (I) of the cantilever, which directly affects its stiffness. U-bar-shaped beams are typically not viable for fabrication using conventional micro-fabrication processes because the formation of such U-bar-shaped structures is prohibitively complex in conventional thin film planar processes. On the other hand, because the silver nanoparticle ink is deposited in a liquid state during the printing process, the printed beam shape can be altered intentionally during the drying process because of the coffee-ring effect, which causes the formation of controllable high ridges in the printed features. In other words, the coffee-ring height can be controlled through choice of appropriate printing and drying conditions to produce U-bar-shaped structures without the need for any additional etching or patterning. Moreover, this unique approach is extremely cost-effective because a U-bar-shaped beam does not require a totally filled beam area, i.e., it can be created by transporting silver nanoparticles from the center to the edges using convective flow, resulting in a highly concentrated silver barrier along the printed cantilever without required use of excessive silver.[17,18] In addition, the moment of inertia, I, and the geometrical dimensions that determine the pull-in and release

[a)]Author to whom correspondence should be addressed. Electronic mail: seungjunc@berkeley.edu.

operations of MEM relays were carefully optimized to obtain operational characteristics that are comparable to those of conventional silicon-based MEM relays. A printed cantilever model was also formulated to accurately estimate the operation of inkjet-printed MEM relays utilizing the coffee-ring effect. The corresponding predictions were verified against stiffness measurements, which were obtained using a nanoindenter, and the results of a 3-dimensional (3D) finite element simulation using COMSOL.

Figure 1 shows the MEM relay fabrication process. A 200 μm wide gate electrode was inkjet-printed using a nanoparticle-based silver ink (CCI-300 from Carbot Corp.) on a silicon/thermally grown silicon dioxide substrate and then sintered at 180 °C for 30 min. A poly(4-vinylphenol) (PVP) solution composed of 10 wt. % PVP and 2 wt. % poly(melamine-co-formaldehyde) used as a cross-linking agent was dissolved in propylene glycol methyl ether acetate (PGMEA) for use in forming the gate dielectric. This PVP solution was spun at 2000 rpm onto the sintered gate electrode and then cross-linked for 30 min on a 200 °C hot-plate, resulting in a film thickness of 530 nm. After the formation of this gate dielectric layer, source and drain electrodes were also inkjet-printed using the same silver ink used for the gate electrode. The gate, source, and drain electrodes had film thicknesses of 380 nm, 305 nm, and 550 nm, respectively. Next, a sacrificial layer was achieved by spin-coating poly(methyl methacrylate) (PMMA, A11 from MicroChem Corp.) at 2000 rpm, resulting in a sacrificial layer film thickness of 1.2 μm. The film was then thermally cured on a 180 °C hot-plate for 10 min. The wetting of the nanoparticle silver ink on the PMMA was enhanced using UV Ozone (UVO) treatment for 3 min. Then, the cantilever beam was printed using the same ink as was used for the electrodes. This was achieved using 5 passes to produce a cantilever with the appropriate thickness and shape. The cantilever was dried at 125 °C for 5 min after each printing process to increase the height of the coffee-ring ridge, and a final coffee ring ridge height of approximately 11 μm was achieved. Note that the width and length of the 5-pass-printed cantilever was 92 μm and 650 μm, respectively. Afterwards, the printed cantilever was sintered at 180 °C using a ramping condition of 5 °C/min. The final actual gap between the drain and the channel was 850 nm because the PMMA sacrificial layer was etched slightly by the silver ink during the cantilever beam printing. After sintering the beam, the anchor region was defined by printing acetone at the cantilever edge to form a via-hole through the PMMA sacrificial layer. Before creating the via-hole, a UVO exposure was used to weaken the PMMA layer, thus enhancing acetone etching. Next, the etched via-hole was filled with inkjetted silver ink to connect the cantilever beam to the source pad. The ink was solidified on a 125 °C hot-plate for 30 min to prevent re-strengthen the PMMA. The anchor structure was then sintered at 180 °C with a ramping condition of 5 °C/min. Finally, the PMMA sacrificial layer was removed by sequential dipping in boiling acetone and isopropyl alcohol (IPA).

Figure 2 shows optical images and cross-sectional profiles of inkjet-printed cantilevers that were fabricated under various printing and drying conditions. Drying after each printing pass produced a large coffee-ring because the printed cantilever edges were pinned to the hydrophobic surface, resulting in a highly concentrated silver barrier with a relatively thin center region, formed following the solvent flow during the drying process. Interspersed drying steps were also used to prevent subsequent printing passes from puddling up to fill the coffee-ring. In other words, we specifically take advantage of the controllability of the coffee-ring to form U-bar-shaped beams; these in turn give advantageous mechanical properties.

The I values for the cantilever were calculated from the measured profiles of printed cantilevers under different drying conditions. As previously mentioned, the height of the coffee-ring (which is denoted by b in the schematic) mainly controlled the I value because the cross-sectional areas of the profiles were nearly equal ($\sim$230 μm^2)[19]

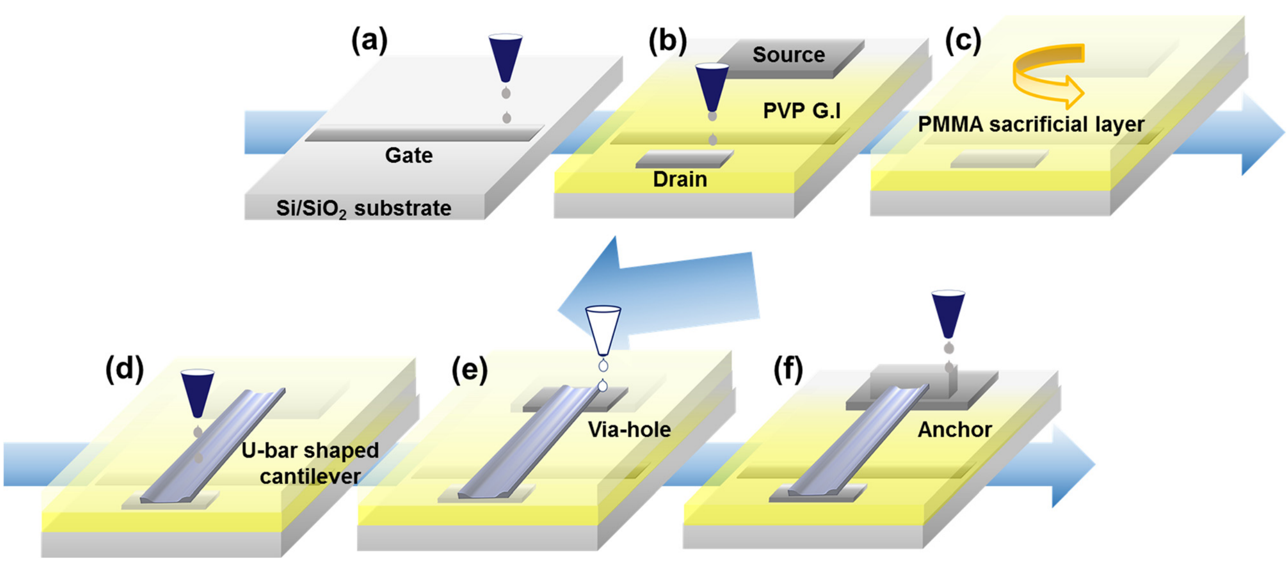

FIG. 1. Process flow for fabricated printed MEM relays: (a) gate electrode printing, (b) source/drain electrode printing on spin-coated PVP gate dielectric, (c) PMMA sacrificial layer deposition, (d) cantilever beam printing, (e) anchor definition via printing-based via-hole formation, and (f) via-hole filling, which is followed by subsequent sacrificial layer removal.

$$I_{Total} = 2\left(\frac{ab^3}{21}\ (\text{for Figure } 2(a))\ \text{or}\ \frac{ab^3}{36}\ (\text{for Figures } 2(b) \text{ and } 2(c)) + Area_A \times dy_A^2\right) + \left(\frac{cd^3}{12} + Area_B \times dy_B^2\right) + \left(\frac{\pi e i^3}{8} + Area_c \times dy_c^2\right)(\text{only for Figure } 2(c)),$$

where a, b, c, and d denote the width and height of the coffee-ring and the flat area on the bottom, respectively. (Note that e and i were only related to $Area_c$ in Figure 2(c) to account for the bump area at the center). This equation was used to calculate the spring constants using values of $K_{eff} = 3E_rI/L^3$ of 4.99 N/m, 0.47 N/m, and 0.09 N/m for Figures 2(a), 2(b), and 2(c), respectively, where E_r and L denote the reduced elastic modulus and the length of the single-clamped cantilever beam, respectively. Herein, E_r of the printed silver cantilever was measured using a nano-indenter (~49 GPa).[8] The calculated k_{eff} value for Figure 2(a) is well-matched with the measured real spring constant of 4.94 N/m (Figure 2(d)). These results show that controlling the coffee-ring effect can dramatically increase the stiffness of printed cantilevers 100-fold over that of flat printed cantilevers with the same cross-sectional area (Figure 2(e)).

To prevent stiction from the capillary force between the cantilever and the drain during the sacrificial layer removal, the sticking force (~4.5 N at a 430-nm displacement in the equation below) should be lower than the elastic force of the cantilever, which is given by $F_{elastic} = kx$, where k and x denote the spring constant and the cantilever displacement, respectively,

$$F_{Sticking} = \frac{2A_{Cantact}\,\gamma \cos\theta_C}{g - x},$$

where $A_{contact}$, γ, θ_C, g, and x denote the contact area between the cantilever and the drain, the surface tension of IPA, the contact angle between IPA and the printed silver electrode, the gap between the cantilever and the drain, and the cantilever displacement, respectively. The weak coffee-ring-free printed cantilevers collapsed easily because of stiction that occurred during the removal of the PMMA sacrificial layer when interspersed drying was not performed for every printing process (Figure 2(e)); this was entirely suppressed for the coffee-ring-enhanced beams.

The relationship between the number of inkjet-printing passes and K_{eff} of the printed cantilever for optimized interspersed drying was also investigated to obtain an adequate cantilever stiffness (Figure 3(a)).[20] As the number of printing passes increases, the coffee-ring height increased linearly up to 18 μm for 8-pass printing. 5-pass-printing delivered sufficient beam stiffness to prevent stiction without increasing the pull-in voltage too much. Under these optimized process conditions, scanning electron microscope images showed strongly suspended cantilever beams without any collapse delivering a constant air gap under 1 μm (Figure 3(b)).

Figure 4(a) shows the measured electrical switching characteristics of the printed MEM relays, including the drain current versus the gate voltage for various drain voltages. An immeasurably low leakage current was obtained due to the air gap between the cantilever and the drain electrode. Excellent switching characteristics were observed, with a pull-in voltage of 6.6 V (V_{PI}) with a near-zero subthreshold swing value. The obtained operational voltage is comparable to that of conventional silicon MEM relays.[9,13,21,22] Figure 4(b) shows the measured drain current

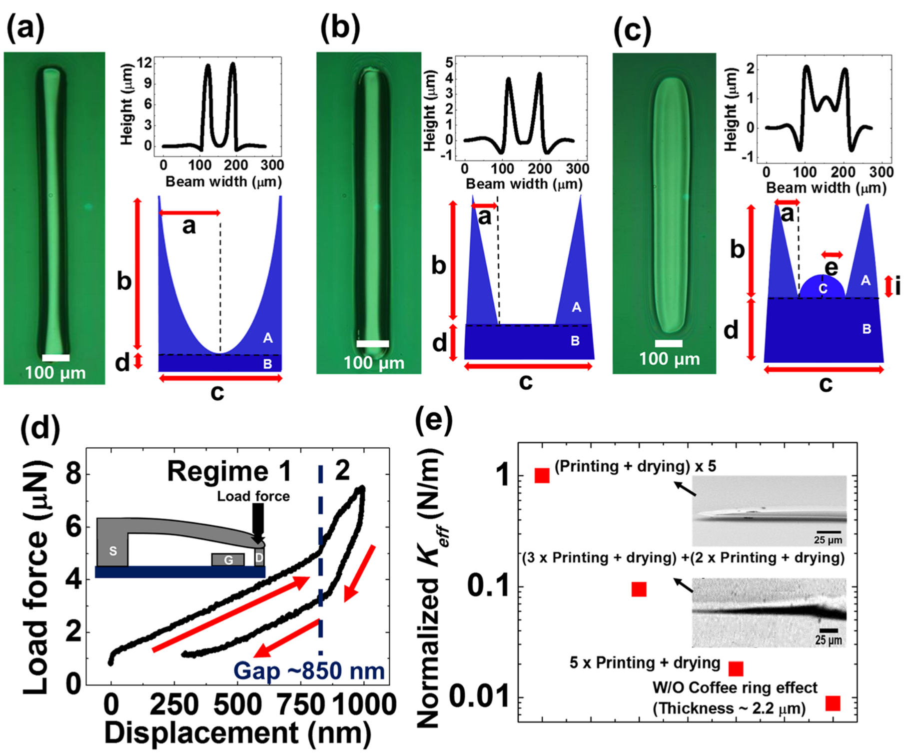

FIG. 2. Optical images, surface profiles, and schematic cross-sections of 5-pass printed silver cantilevers, with: (a) drying after ever printing pass, (b) drying only twice over the 5 passes, and (c) without interspersed drying on a 125 °C hot-plate. (d) Displacement versus applied force curve of the printed cantilever beam as measured by nanoindentation. From the regime 1, spring constant (k_{eff}) could be extracted based on the fact that $F = k_{eff}$ x(= displacement). (e) Normalized cantilever beam stiffness under various drying conditions (SEM images of suspended and collapsed cantilever are shown in the inset).

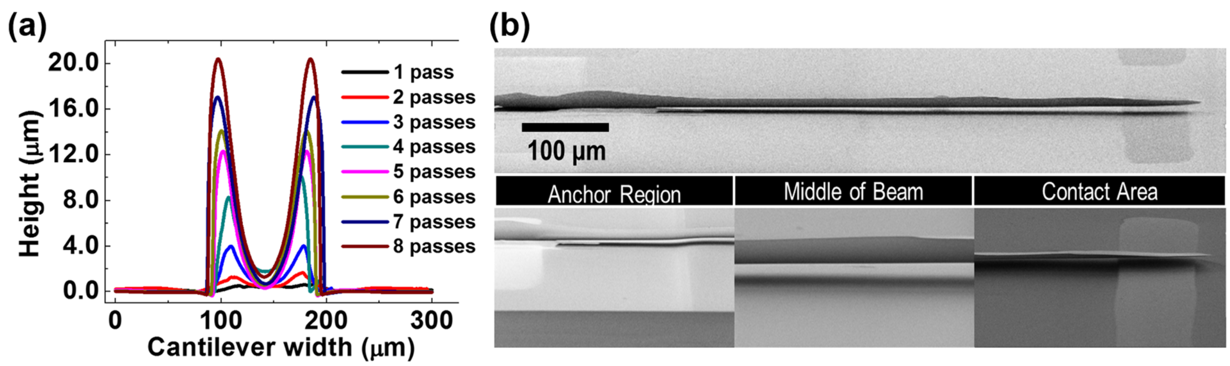

FIG. 3. (a) Profiles of printed cantilevers on PMMA for varying numbers of printing passes. (b) SEM images of MEM relay with 5-pass-printed cantilever beam (close-up images are also shown).

versus the drain voltage for a fixed V_{GS} of 10 V. The on-resistance (R_{ON}) consisted of two components (a metal-metal contact resistance between the cantilever and the drain electrode and the channel resistance): the I_{DS} increased linearly with the V_{DS}, which corresponded to a R_{ON} value of 14.3 Ω for $V_{GS} > V_{PI}$.

A simulation was also performed with COMSOL Multiphysics to verify the operation of the U-bar-shaped MEM relay. In this simulation, the dimensions of the printed U-bar-shaped cantilever beam and the bottom electrodes were defined based on the measured dimensional parameters and Young's modulus. The electrostatic force density associated with the Maxwell stress tensor is given as follows:

$$F = -0.5\,(E \cdot D)n + (n \cdot E)D^T,$$

where *E, D, and n* denote the electrical field, the electric displacement vector, and the outward normal vector, respectively. The curve of the displacement versus the cantilever position was used to determine the V_{PI} when the induced electrostatic force exceeds the elastic force of the cantilever, pulling the cantilever down (Figure 4(c)). The gap between the cantilever and the drain was matched to that measured experimentally via the aforementioned nanoindentation measurement; the voltage required to cause the cantilever to traverse this distance is then the simulated pull-in voltage. Figure 4(d) shows images of the deformed cantilever along the *xz*-plane as a function of the applied electrical potential: the cantilever began to touch the drain when the applied voltage exceeded 6.6 V. The V_{PI} value obtained from the simulation results matched the experimental value well. The simulation results also shows that the mechanical stiffness of the printed U-bar-shaped cantilever is equal to that of a flat cantilever with a thickness of 10.23 μm, while using significantly less silver.

In conclusion, we realized strongly suspended U-bar-shaped cantilever beams by exploiting the coffee-ring effect for high-performance printed MEM relays. By using optimized multi-pass printing and interspersed drying, we controlled the height of the coffee-ring ridge to change the

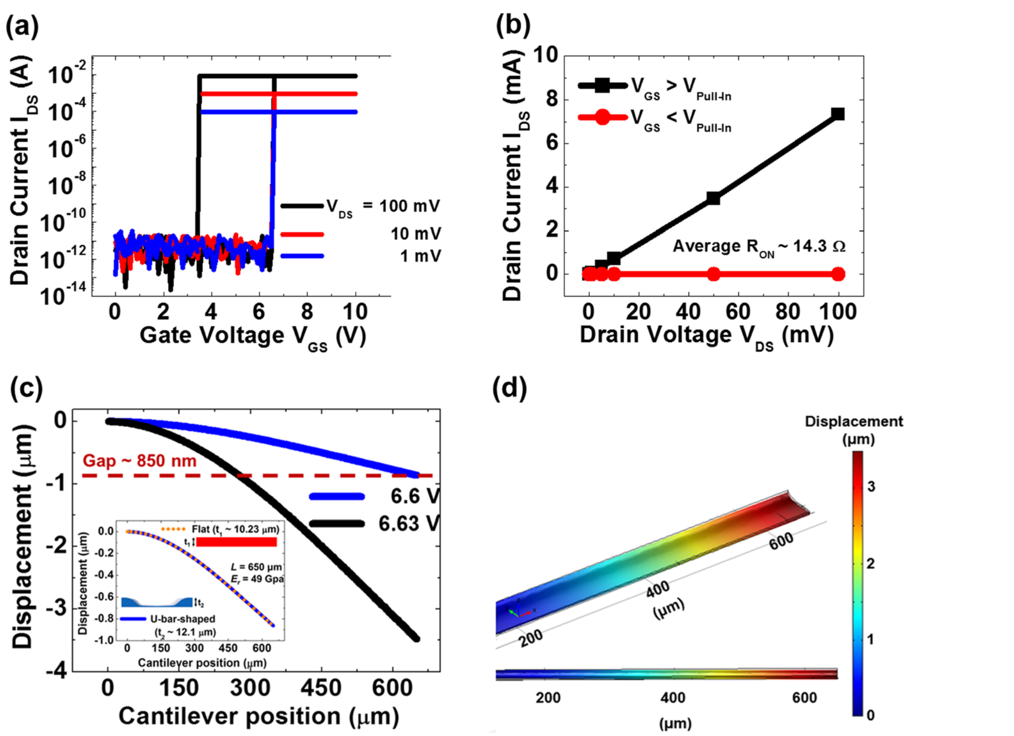

FIG. 4. (a) Switching characteristics of MEM relay with 5-pass-printed cantilever beam for various V_{DS} values and (b) I_{DS}-V_{DS} characteristics of MEM relay (on-state resistance is also extracted). (c) Analysis of displacement using COMSOL Multi-physics to verify V_{PI} (Comparison of displacements for flat and U-bar-shaped cantilevers by simulating with COMSOL is also included in inset. The calculated K_{eff} of the 5-pass-printed U-bar-shaped cantilever was equal to that of a flat cantilever with a thickness of 10.23 μm), (d) graphical results of displacement at a gate voltage of 6.63 V.

cantilever stiffness. The coffee-ring effect was used to obtain an effective thickness of over 10 μm while using minimal silver. This unique approach is an easy, rapid, and low-cost process that delivers a mechanically enhanced and stable MEM relay with excellent performance. Experimentally derived stiffness values were consistent with mechanical measurements performed using indentation and the results of a simulation performed using 3D finite difference methods. We believe the coffee-ring enhanced MEM relays in this work provide an attractive path for realization of ultra-low-cost and energy efficient MEM applications.

This work was supported in part by Systems on Nanoscale Information fabriCs (SONIC), one of the six SRC STARnet Centers, sponsored by MARCO and DARPA.

[1] A. C. Arias, J. Daniel, B. Krusor, S. Ready, V. Sholin, and R. Street, J. Soc. Inf. Disp. **15**, 485 (2007).
[2] T. Kawase, T. Shimoda, C. Newsome, H. Sirringhaus, and R. H. Friend, Thin Solid Films **438**, 279 (2003).
[3] V. Subramanian, J. M. J. Frechet, P. C. Chang, D. C. Huang, J. B. Lee, S. E. Molesa, A. R. Murphy, D. R. Redinger, and S. K. Volkman, Proc. IEEE **93**, 1330 (2005).
[4] L. Yang, A. Rida, R. Vyas, and M. M. Tentzeris, IEEE Trans. Microwave Theory Tech. **55**, 2894 (2007).
[5] S. Chung, M. Jang, S.-B. Ji, H. Im, N. Seong, J. Ha, S.-K. Kwon, Y.-H. Kim, H. Yang, and Y. Hong, Adv. Mater. **25**, 4773 (2013).
[6] A. Valletta, A. Daami, M. Benwadih, R. Coppard, G. Fortunato, M. Rapisarda, F. Torricelli, and L. Mariucci, Appl. Phys. Lett. **99**, 233309 (2011).
[7] S. H. Kim, K. Hong, W. Xie, K. H. Lee, S. Zhang, T. P. Lodge, and C. D. Frisbie, Adv. Mater. **25**, 1822 (2013).
[8] E. S. Park, Y. Chen, T.-J. K. Liu, and V. Subramanian, Nano Lett. **13**, 5355 (2013).
[9] K. Akarvardar, D. Elata, R. Parsa, G. C. Wan, K. Yoo, J. Provine, P. Peumans, R. T. Howe, and H.-S. P. Wong, IEEE International Electron Devices Meeting (IEDM) Tech. Dig. **2007**, 299.
[10] J. M. Bustillo, R. T. Howe, and R. S. Muller, Proc. IEEE **86**, 1552 (1998).
[11] S.-D. Ko, J. O. Lee, H.-H. Yang, M.-W. Kim, Y.-H. Song, and J.-B. Yoon, Appl. Phys. Lett. **99**, 113516 (2011).
[12] H. Kam and T.-J. K. Liu, IEEE Trans. Electron Devices **56**, 3072 (2009).
[13] T.-J. K. Liu, J. Jeon, R. Nathanael, H. Kam, V. Pott, and E. Alon, IEEE International Electron Devices Meeting (IEDM) Tech. Dig. **2010**, 424.
[14] V. Bromberg, S. Ma, and T. J. Singler, Appl. Phys. Lett. **102**, 214101 (2013).
[15] D. Redinger, S. Molesa, S. Yin, R. Farschi, and V. Subramanian, IEEE Trans. Electron Devices **51**, 1978 (2004).
[16] D. Soltman and V. Subramanian, Langmuir **24**, 2224 (2008).
[17] P. J. Yunker, T. Still, M. A. Lohr, and A. G. Yodh, Nature **476**, 308 (2011).
[18] R. D. Deegan, O. Bakajin, T. F. Dupont, G. Huber, S. R. Nagel, and T. A. Witten, Nature **389**, 827 (1997).
[19] J. M. Gere and B. J. Goodno, *Mechanics of Materials* (CL-Engineering, 2013).
[20] S. Pamidighantam, R. Puers, K. Baert, and H. A. C. Tilmans, J. Micromech. Microeng. **12**, 458 (2002).
[21] J. Jeon, R. Nathanael, V. Pott, and T.-J. K. Liu, IEEE Electron Device Lett. **31**, 515 (2010).
[22] R. Nathanael, V. Pott, H. Kam, J. Jeon, and T.-J. K. Liu, IEEE International Electron Devices Meeting (IEDM) Tech. Dig. **2009**, 223.